RESEARCH ARTICLE

Deregulation of miR-10b and miR-21 Correlate with Cancer Stem Cells Expansion through the Apoptotic Pathway in Prostate Cancer

Kamla Kant Shukla[1]*, Gautam Ram Choudhary[2], Shrimanjunath Sankanagoudar[1], Sanjeev Misra[3], Jeevan Ram Vishnoi[4], Puneet Pareek[5], Kiran Kumar Pilla[1], Sachchida N. Pandey[6], Praveen Sharma[1]

Abstract

   Background: MicroRNAs are small, non-coding RNA molecules that regulate important cellular processes such as tumorigenesis, cell proliferation, and apoptosis. Cancer stem cells are a subset of cells that control metastasis and cell proliferation. In this study, we focus on the roles of miR-10b, miR-21 and correlate with cancer stem cells through the apoptotic pathway in different stages of prostate cancer (PCa). **Methods:** In total, 45 patients, each group with Benign prostatic hyperplasia (BPH), localised PCa, and metastatic PCa, were recruited. MicroRNA and gene expression were estimated through quantitative polymerase chain reaction. Flow cytometry was used to characterise prostate cancer stem cells (PCSCs), estimate reactive oxygen species (ROS), apoptosis and chemiluminescent immunoassay was used to estimate interleukin 6 (IL-6), tumour necrosis factor (TNF-α), prostate-specific antigen (PSA), and testosterone. **Results:** The fold change mean expressions of miR-21, miR-10b, Cytochrome C, and B-cell lymphoma 2 (BCL-2) were significantly upregulated in localised and metastatic PCa compared with BPH. In contrast, the mean fold change expressions of Bcl-2-associated X protein (BAX), Caspase-3, Caspase-9, and Second mitochondria-derived activator of caspase (SMAC) were lower in localised and metastatic PCa compared to BPH. The levels of IL-6, TNF-α, ROS, PSA and testosterone also showed a significant increase while apoptosis was decreased in both localized PCa and metastatic PCa as compared with BPH. In bioinformatics analyses, we found a similar pattern of miRNAs and gene expression in PCa databases. Our study also found a high expression of CD44+/CD24- and CD44+/CD133+ in localised and metastatic PCa compared with BPH. **Conclusion:** Our findings suggest miR-10b and miR-21 promote PCSCs and may target apoptotic genes involved in PCa pathogenesis; these miRNAs could be used as diagnosis biomarkers of PCa. In PCa pathogenesis and PCSCs regulation, the interaction between these two players is crucial and will help develop new PCa therapeutic targets.

   Keywords: miRNAs expression- Prostate cancer stem cell- apoptotic pathway mRNA expression- Diagnostic

Introduction

   Prostate cancer (PCa) is one of the most prevalent cancers in men worldwide. It ranks second in the frequency of cancers encountered, with an estimated incidence of 1.3 million and ranks fifth in male mortality (Siegel et al., 2020). Approximately 241,000 PCa cases were diagnosed in the United States alone, and 29,430 PCa-related deaths were recorded in 2020 (Bray et al., 2018). The projected incidence of PCa in Asia is 4.4 per million people, and the fact that this will cause substantial morbidity soon is a matter of great concern (Mathur et al., 2020). Despite much advancement in the treatment regimen for PCa, identifying and treating this disease remains challenging (Sharifi et al., 2017). Numerous PCa biomarkers are available for diagnosis and precise prognosis. However, the real challenge is to identify those markers that are helpful for early clinical diagnosis and validate these markers and relevant technologies for clinical application (Shukla et al., 2017). Cancer stem

[1]Department of Biochemistry, All India Institute of Medical Sciences, Jodhpur, Rajasthan, India. [2]Department of Urology, All India Institute of Medical Sciences, Jodhpur, Rajasthan, India. [3]Department of Surgical Oncology, Atal Bihari Vajpayee Medical University, Lucknow, India. [4]Department of Surgical Oncology, All India Institute of Medical Sciences, Jodhpur, Rajasthan, India. [5]Department of Radiation Oncology, All India Institute of Medical Sciences, Jodhpur, Rajasthan, India. [6]Department of Pathology (Transplant Immunology and Genetics) Muljibhai Patel Urology Hospital, Dr. Virendra Desai Road, Nadiad Gujarat-387001 India. *For Correspondence: shukla.kgmu@gmail.com

cells (CSCs) are a subpopulation of tumor cells that can drive tumor initiation and cause relapses (Zuoren et al., 2012). Due to their importance, several biomarkers that characterize CSCs have been identified and correlated to diagnosis, therapy, and prognosis (Abrahamsson et al., 1999). The CSCs were identified and isolated using different cell surface markers and transcription factors (Gao et al., 2019). Many markers have been placed in PCa, such as CD24, CD44, CD133, CD166, and α2β1 integrin (Sharifi et al., 2017). However, the ideal combination that could result in the distinction of cancer stem cells has not been found yet, because of PCa genetic heterogeneity.

Recent studies have offered insight into microRNAs (miRNAs), allowing the understanding of the governing mechanisms of several cancers, including PCa (Raue et al., 2021; Carthew et al., 2009). There are two different forms of miRNA: tumour suppressor miRNA and oncogenic miRNA. Both play different roles in regulating the carcinogenesis process (Rupaimoole et al., 2017). So, these miRNAs can be employed as biomarkers and may offer a potential role in early illness identification and disease progression intervention. However, people may respond differently to therapy depending on their miRNA levels and effectiveness. MiR-10b appears to play a pro-tumorigenic, pro-metastatic role in several cancer types, such as breast, prostate, and endometrial cancers, due to its role in epithelial-mesenchymal transition and metastasis (Patrick et al., 2018). Similarly, a few other studies have also reported the upregulation of miR-21 in various cancers, including PCa (Ribas et al., 2010). miRNAs have been shown to alter the signaling cascade that facilitates the stemness potential of CSCs, leading to self-renewal, proliferation, invasiveness (epithelial to mesenchymal transition), resistance, and recurrence in cancers (Khan et al., 2019). Several reports have identified molecular surface markers for Prostate Cancer stem cells (PCSCs) such as CD44, CD133, CD24, CD40, and α2β1 that are significantly associated with poor prognosis in PCa (Mei et al., 2019; Yun et al., 2016; Patrawala et al., 2006). However, the mechanisms by which miRNAs regulate the stemness characteristics of PCSCs are still unclear.

The clinical relevance and biological function of miR-10b and miR-21 have been linked to several cancers via altered gene expression in the apoptotic pathway (Patrick et al., 2018; Ribas et al., 2010). However, their association with cancer stem cells in PCa has yet to be investigated. In PCa, the hormone-resistant, the metastatic phenotype is allied with the anti-apoptotic BCL-2 (B-cell lymphoma 2) gene expression, with a concomitant increase in the Gleason score (Hering et al., 2001). In addition, PCa development is also influenced by cytokines like interleukin (IL)-6 and tumor necrosis factor (TNF)-α (Michalaki et al., 2004). Several studies have reported significantly elevated serum IL-6 levels in patients with advanced hormone-refractory PCa (Michalaki et al., 2004). More recently, Culig Z et al. (2021) revealed elevated IL-6 levels involved in the development or progression of PCa. Several studies have found that the inflammatory cascade, including reactive oxygen species (ROS), apoptosis, and cell cycle differentiation, play important roles in PCa progression (Westaby et al., 2021). High levels of ROS in

cancer cells can be caused by increased metabolic activity, mitochondrial dysfunction, increased cellular receptor signaling, and oncogene activity (Xiao et al., 2018).

Several recent studies have reported the most relevant miRNAs involved in PCa biology and have established a PCa-specific miRNA expression profile (Raue et al., 2021; Patrick et al., 2018). In this study, we sought to analyze the expression of miR-10b, miR-21, and genes expression in the apoptotic pathway along with cancer stem cells and thus correlated them with the cytokine, apoptosis, ROS, testosterone, and PSA levels observed in different stages of PCa. Here, we present the survival analysis considering the regulatory relationships of miRNAs and their target genes through the cancer genome atlas (TCGA).

Materials and Methods

Sample Collection

This study was conducted in the Departments of Biochemistry and Urology at the All-India Institute of Medical Science (AIIMS), Jodhpur, India, after receiving ethical approval from the AIIMS Institutional Ethics Committee. Each subject gave written informed consent after accepting a thorough written and verbal explanation of the study. The untreated and newly diagnosed potential participants were included in the study. Subjects who underwent elective surgery at AIIMS Jodhpur were enrolled in the study. The patients who had concurrent cancer at any other site were excluded from the study. Tissue and blood sample were collected from each diagnosed localised PCa, metastatic PCa, and benign prostatic hyperplasia (BPH) patient. The carcinoma samples were assessed through histological examination. The BPH samples were taken from individuals who had undergone prostatectomy or cystoprostatectomy, and the specimens were histologically proven to be free of cancer cells and stored at -800C. A detailed demographic, clinical history, and other relevant patient information were recorded. The study included 45 subjects from each group (BPH patients, localised PCa, and metastatic PCa); figure 1 depicts a detailed work flowchart.

RNA Extraction and Complementary DNA Synthesis

The modified acid guanidinium thiocyanate-phenol-chloroform (AGPC) technique was utilized to extract total RNA from PCa and BPH. Trizol reagent (Invitrogen Life Technologies) was used for the procedure. The Affinity Script qPCR First-strand cDNA synthesis kit (Agilent Technologies, USA) was used to synthesize cDNA using oligo dT adapter primer specific to reference genes (RNU6) and reverse transcriptase. The oligo-dT adapter primer consisted of a unique sequence at it 5'end, which allowed the amplification of cDNA by qRT-PCR (Alvarez et al., 2014).

Expression of miRs and mRNAs by quantitative real-time PCR (qPCR)

The qRT-PCR was performed using Power Master Mix SYBR Green (Alvarez et al., 2014) (Thermo Fisher, Waltham, MA) following the protocol: 2 minutes at 94°C at the start, followed by 38 cycles of the 20s each at 94°C,
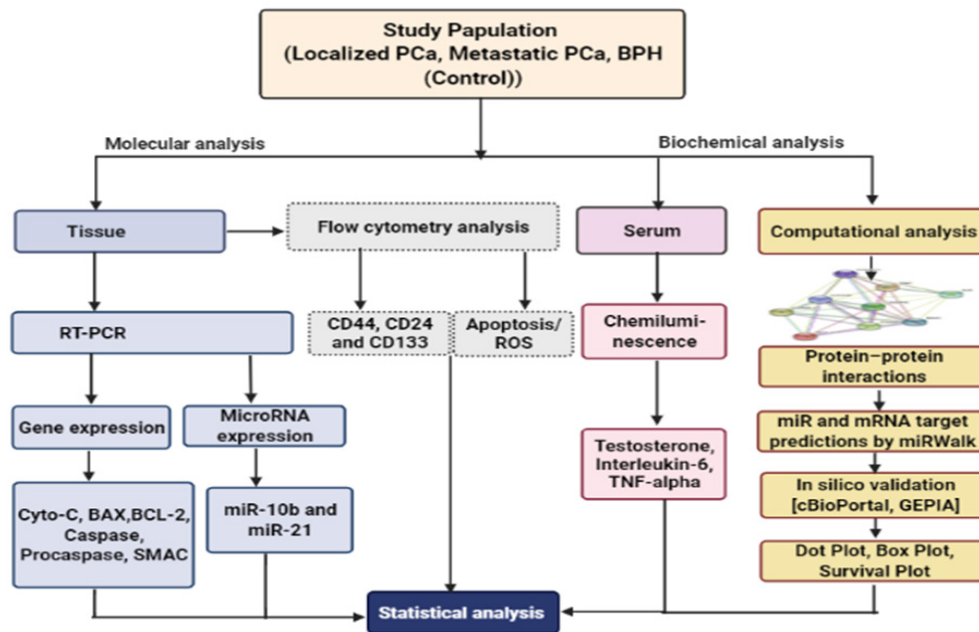
Figure 1. Workflow of the Study

then 30 s at 60°C, and 1 minute at 72°C, succeeded by a dissociation stage. The inverse log of the delta/delta CT was used to calculate the relative expression; miRNA expression was normalised to U6 expression, while mRNA expression was normalised to GAPDH expression. (Standard reference) to analyse the fold change in mRNA expression (Livak et al., 2001). Melting curves were examined to ensure the expected RT-qPCR product was correctly amplified. The results were expressed as the mean fold change in two groups (localized and metastatic PCa), and the relative expression was calculated using $2-(\Delta CT)$ (list of primers see in supplementary Table 1).

Characterization of stem cells by flow cytometry

Five grams of PCa tissue were finely chopped into small pieces using surgical scissors, and all details pieces were collected into a 10 mL stripette fast. Further, it was resuspended in a 15 mL digestion buffer and incubated for 4 hours at 37°C. After centrifugation for 5 minutes at 1,800 rpm at 37°C, single cells were washed twice with 25ml of Phosphate-buffered Saline PBS), and suspended again in 5 ml 0.25% TrypLE. After treatment with 15ml of DMEM + 10% FBS, and centrifugation at 1800 rpm, the pellet was reconstituted and passed through different gauge needles (18, 20, and 22). After that, the cells were passed through a 100 mm filter and washed with DMEM+10% FBS. The filtered cells were centrifuged at 1,800 rpm, reconstituted in DMEM with 10% FBS, and filtered again using a 40 mm filter Afterwards, the cells were resuspended in fresh 10 mL DMEM+10% FBS and centrifuged at 1,800 rpm. FITC anti-human CD24 (Anti-CD24-FITC, Invitrogen, Carlsbad, CA, USA), PE anti-human CD44 (anti-CD44-PE and anti-human CD133 (anti-CD133-PE), Invitrogen, Biosciences, California, USA) were used to stain 1 million filtered cells for 15 minutes at 4°C in 100ul of stain solution. Fluorescence-activated cell sorting was used throughout the investigation on a BD FACS CantoTM II flow cytometer (FACS). A minimum

of 10,000 occurrences were recorded for each sample run. To analyse gates, unstained control cells, isotype-specific control stains, and single stains were used (BD Biosciences). The dot plot forwards scatters (FSC) vs side scatter (SSC) was used to eliminate dead cells and debris (Hurt et al., 2008).

Hormonal Assay

The serum testosterone levels and Prostate-specific antigen (PSA) levels were measured using an automated chemiluminescent immunoassay (Morote et al., 2010).

Estimation of IL-6 and TNF-α

IL-6 and TNF-α levels in the blood were measured using a highly sensitive indirect sandwich enzyme-linked immunosorbent assay (Bender MedSystems, Austria).The reaction was stopped with the addition of acid, and the absorbance was measured at 450 nm. The limits of detection were 1.4 pg/ml and 3.83 g/ml, for IL-6 and TNF-α, respectively. For IL-6 and TNF-α, the overall inter-assay coefficients of variance were 5.2 percent and 6.9 percent, respectively. According to the manufacturer's recommendations, all IL-6 and TNF-α tests were duplicated in the same batch. The serum levels of IL-6 and TNF-α were provided as a normal distribution (Shukla et al., 2013).

Apoptosis assay

Flow cytometry was used to examine the distribution of apoptotic and necrotic cells in the control and patient groups using annexin-V, a phospholipid-binding protein and propidium iodide (PI) uptake. The fluorescence of FITC was estimated using an FL-1 (530 nm) and PI using an FL-2 (585 nm) filter, and 10,000 events were recorded on a BD flow cytometer (Becton-Dickinson, USA) (Vermes et al., 1995).

Total ROS measurement

The reactive oxygen species (ROS) levels were evaluated in both BPH and patient groups. To construct the standard ROS profile for each group of individuals, one sample from each patient group was chosen. 2,7- dichlorfluoresce in diacetate was used to measure ROS production (DCFH-DA) in the BD flow cytometer (Becton-Dickinson, USA) (Vermes et al., 1995).

Bioinformatics target predictions

We used miRWalk 2.0 to predict information about potential binding sites among genes (including the entire sequence) and miRNAs derived from the TarPmiR algorithm. The miRWalk database contains information generated by TarPmiR, a prediction tool for miRNA-mRNA binding sites that can use CLASH miRNA-mRNA binding experiment data (Sticht et al., 2018). The cBioPotal for Cancer Genomics database evaluated the frequency of gene alterations (such as mutations, deletions, copy number gains, and amplifications) in PCa prognostic regulators. We find out the expression of our genes of interest from cBioPotal and GEPIA for bioinformatics validation of the study (Unberath et al., 2022; Tang et al., 2017). The TCGA database contains high-throughput sequencing data and prognostic data. Linked Omics was used to analyze omics data in cancer. We measured the receiver operating characteristic (ROC) curve for overall survival between risk patients, stratified by CancerMIRNome (http://bioinfo.jialab-ucr. org/CancerMIRNome/, accessed on 31 October 2022) and miRNACancerMAP database (http:/cis.hku.hk/ miRNACancerMAP /quicksearch.php).

Protein-Protein Interaction Network Construction and Correlation Analysis

Protein-protein interactions (PPI) have been studied using the Search Tool for the Retrieval of Interacting Genes (STRING) database. There were only a pair of PPI couples that scored higher than 0.400. To visualize the PPI network. It is vital to highlight that nodes with a high degree of interconnection are more critical to the overall network stability (Szklarczyk et al., 2021).

Statistical analysis

The data were summed together as mean SD (standard deviation). Independent Student's t-test was used to assess marker expressions (i.e., relative fold change vs. BPH control) across two groups (localised and metastatic PCa). A Pearson correlation analysis was used to determine the relationship between the makers. The markers' diagnostic accuracy (sensitivity and specificity) was analyzed by Receiver operating characteristic (ROC) curve. Statistical significance was a two-tailed (=2) $p<0.05$. SPSS software was used to conduct the analyses (Windows version 22.0).

Results

Demographics

The study included 135 patients of three different groups such as BPH patients, localised PCa, and metastatic PCa, ranging in age from 40 to 77 years, and all the clinical and demographic features such as age, stages, histopathological status, PSA levels, and Gleason score were depicted in Table 1.

Target predictions

TarPmiR used a random-forest-based technique to predict miRNA target sites to combine 6 traditional and 7 recent features. Hence based on this approach, we have identified common apoptosis-regulating proteins that have probable binding sites for miR-10b and miR-21b. The outcome of miRWalk 2.0 is shown in Table 2.

MiRNA and mRNA expressions

The marker expressions of three groups (BPH, localised and metastatic) PCa is summarised in Figure 2. In this study, the tissue levels of miR-21 and miR-10b were significantly upregulated in both groups of PCa patients with mean fold change in localised (1.21±0.50), (1.47±0.53) and metastatic PCa (1.32±0.59), (1.61±0.48) than in BPH. The apoptotic pathway genes expression

Table 1. Demographic Characteristics of PCa Patients

Variables	N (%)	Age	PSA levels	Gleason score
Histological grade				
BPH	45 (33.33)	62.75 ± 4.85	8.42 ± 1.25	3.02 ± 0.82
Localised PCa	45 (33.33)	64.84 ± 5.73	88.59 ± 37.28	4.05 ± 0.88
Metastatic PCa	45 (33.33)	66.89± 6.34	87.28 ± 10.99	4.58 ± 0.50

Table 2. Target Predictions of miR-10b and miR-21

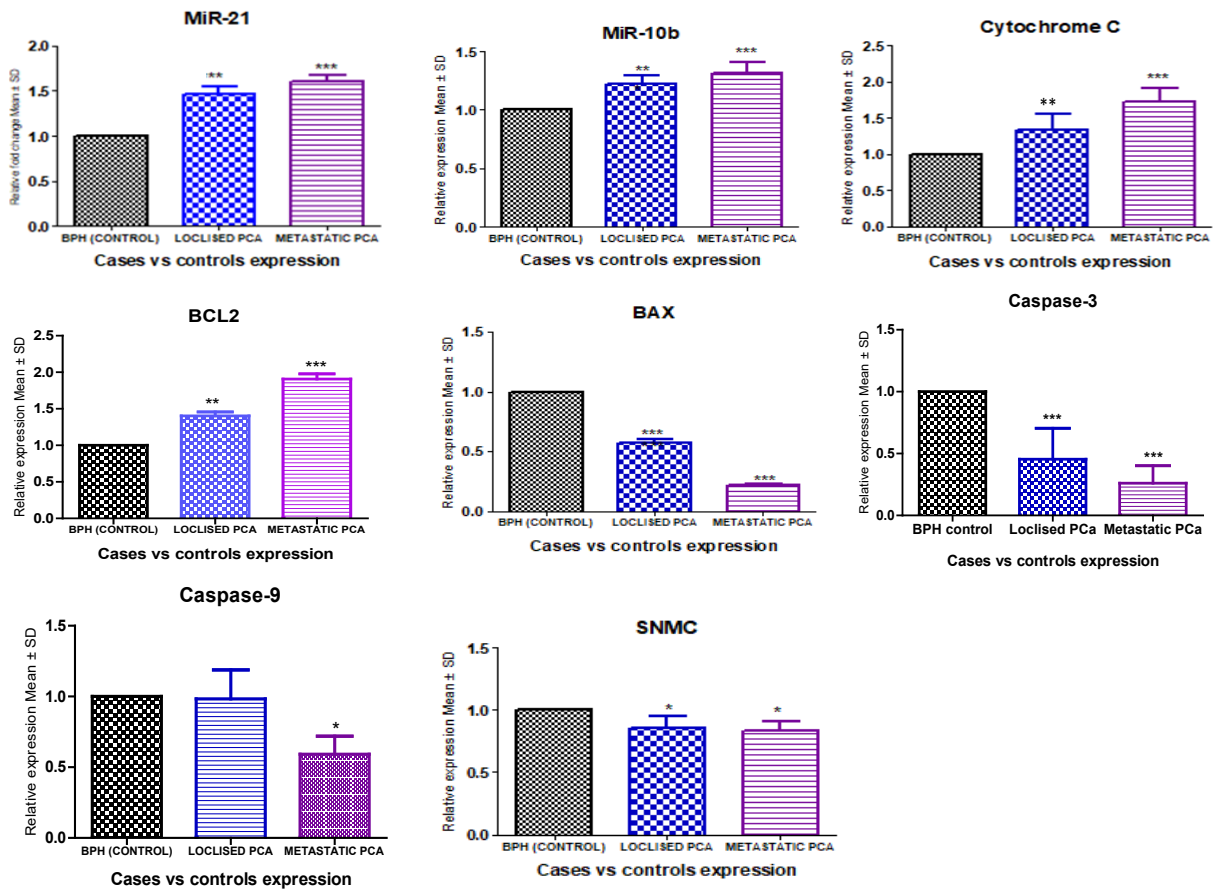| miRNA	Target Gene	Binding region Length	Binding Site
hsa-miR-10b-5p	BCL2	17	3`UTR
	PARP	24	CDS
	PAX	17	3`UTR
hsa-miR-21-5p	BCL2	15	CDS
	PARP	12	CDS
	PAX	19	CDS

Figure 2. The Histogram Shows miRNA and mRNA Fold Change Expression in Tissue Samples of PCa Patients (Localised and Metastatic) Compared with BPH Patients. B). The heatmap depicts the fold change expression of the apoptotic genes studied in PCa. (Blue to yellow colour represents gradually increased fold change expression). *- P < 0.05, **- P < 0.01,***- P < 0.001

Cytochrome C and BCL2 were comparatively higher in both localised and metastatic (p<0.05) PCa groups as compared to BPH. In contrast, fold change mean expressions of BAX, Caspase-3, Caspase-9 and SMAC significantly decreased in both localised and metastatic PCa (p<0.001) compared to BPH. Comparing the fold change mean expressions of the two groups shows a statistically significant difference in miR-10b, miR-21, BCL2, Caspase-3, BAX and caspase-9 while SMAC did not show a significant difference in metastatic PCa as compared to localised PCa. Subsequently, our mRNA expression results indicated a similar pattern to the cBioPortal's online database (Figure 5, 6).

PSA score and Gleason grade
The PSA score and Gleason grade of three groups (BPH control, localised PCa and metastatic PCa) is summarised in table 1. The mean PSA score and Gleason grade were comparatively higher in both localised PCa and metastatic PSA compared to the BPH control. On comparing, ANOVA showed significantly different PSA scores (F=218.60, p<0.001) and Gleason grades (F=53.37, p<0.001) among the groups. Further, the Tukey test showed that the mean PSA score and Gleason grade were significantly (p<0.001) higher in both localised PCa and metastatic PCa as compared to BPH control

in table 3. Further, the Gleason grade was also found to be significantly (p<0.01) different and upregulated in metastatic PCa compared to localised PCa. However, the mean PSA score did not (p>0.05) differ between localised PCa and metastatic PCa was found to be statistically the same.

Reactive oxygen species
The mean ROS concentration was significantly (p<0.001) higher in both localized PCa (24.1%) (52.24±6.02) and metastatic PCa (41.3%) (69.41±5.65) as compared to BPH control (28.15±3.84). Further, it was also found significantly (p<0.001) different and upregulated (17.2%) in metastatic PCa in comparison to localized PCa (Figure 3).

Apoptosis level
The mean number of total apoptotic cells (early + late) was significantly decreased (p<0.001) in both localised PCa (1.870.50) and metastatic PCa (2.84 ±1.07) compared to BPH control (0.57±0.21). Furthermore, it was observed (p<0.001) to be significantly different and decreased (34.1%) in metastatic PCa when compared to localised PCa (Figure 3).

Kamla Kant Shukla et al

Table 3. Intercorrelations of Marker Expression in Patients of Localised PCa (n=45) by Pearson Correlation Analysis

	AGE	PSA	GLEASON GRADE	TNF-α	IL-6	ROS	Apoptosis	Testosterone	miR 21	miR 10b	Cyto C	BCL2	BAX	Caspase	Procaspase	SMAC
AGE																
PSA	0.322* (0.031)															
GLEASON GRADE	-0.032 (0.833)	0.232 (0.126)														
TNF-α	-0.078 (0.610)	-0.008 (0.958)	-0.017 (0.910)													
IL-6	0.36* (0.014)	0.361* (0.015)	0.022 (0.884)	-0.015 (0.923)												
ROS	-0.019 (0.903)	-0.121 (0.429)	0.174 (0.252)	0.178 (0.242)	0.057 (0.708)											
Apoptosis	0.137 (0.368)	0.286 (0.057)	0.126 (0.409)	0.012 (0.938)	-0.074 (0.631)	-0.177 (0.244)										
Testosterone	-0.151 (0.323)	0.148 (0.331)	0.181 (0.235)	-0.031 (0.841)	-0.034 (0.824)	-0.259 (0.085)	0.268 (0.075)									
miR 21	-0.115 (.452)	0.042 (0.786)	-0.026 (0.865)	0.092 (0.546)	0.113 (0.461)	-0.272 (0.071)	0.372 (0.012)	0.223 (0.141)								
miR 10b	-0.088 (0.566)	-0.219 (0.148)	-0.222 (0.143)	-0.153 (0.316)	-0.063 (0.68)	-0.306* (0.04)	-0.146 (0.337)	0.077 (0.614)	0.149 (.328)							
Cyto C	-0.170 (0.26)	-0.223 (0.14)	-0.149 (0.32)	0.101 (0.51)	-0.099 (0.51)	-0.008 (0.96)	0.107 (0.48)	0.117 (0.44)	0.328* (0.27)	0.078 (0.61)						
BCL2	0.026 (0.86)	-0.162 (0.28)	-0.115 (0.45)	-0.052 (0.73)	0.020 (0.89)	-0.238 (0.11)	-0.298* (0.04)	-0.018 (0.90)	0.036 (0.81)	0.256 (0.08)	0.048 (0.75)					
BAX	-0.100 (0.515)	-0.007 (0.96)	0.115 (.451)	0.039 (0.798)	-0.110 (0.471)	0.031 (0.841)	0.098 (0.521)	0.018 (0.907)	-0.037 (0.811)	0.161 (0.291)	-0.127 (0.407)	-0.128 (0.40)				
Caspase	0.032 (0.83)	0.057 (0.70)	-0.301* (0.024)	-0.191 (0.20)	0.030 (0.84)	0.034 (0.82)	-0.087 (0.57)	-0.277 (0.06)	-0.150 (0.32)	-0.019 (0.90)	0.310* (0.03)	-0.128 (0.40)	0.062 (0.68)			
Procaspase	-0.058 (0.706)	-0.126 (0.40)	0.100 (0.512)	0.187 (0.22)	-0.075 (0.625)	0.169 (0.267)	-0.016 (0.914)	-0.040 (.793)	-0.129 (0.397)	-0.116 (0.446)	0.085 (0.581)	0.209 (0.16)	-0.054 (0.72)	-0.024 (0.87)		
SMAC	0.061 (0.68)	-0.280 (0.06)	-0.127 (0.40)	-0.203 (0.18)	0.036 (0.81)	0.137 (0.37)	0.053 (0.72)	-0.190 (0.21)	0.053 (0.72)	0.135 (0.37)	-0.172 (0.25)	0.209 (0.16)	-0.016 (0.91)	0.057 (0.70)	0.253 (0.02)	

Computed correlation used Pearson-method with listwise-deletion; *- P < 0.05, **- P < 0.01

Table 4. Intercorrelations of Marker Expression in Patients of Metastatic PCa (n=45) by Pearson Correlation Analysis

|	Age	PSA	Gleason G	ROS	apop	Testo	TNF-α	IL-6	miR21	miR10b	Cyt-c	BCL2	BAX	Caspase	Procaspase	SMAC
Age	1															
PSA	0.169 (0.27)	1														
Gleason	-0.095 (0.537)	0.292* (0.01)	1													
ROS	0.091 (0.552)	-0.16 (0.295)	0.175 (0.252)	1												
Apoptosis	0.068 (0.656)	0.345* (0.02)	0.079 (0.604)	0.286* (0.05)	1											
Testosterone	-0.243 (0.108)	-0.007 (0.964)	-0.006 (0.966)	0.039 (0.797)	0.014 (0.928)	1										
TNF-α	0.02 (0.897)	0.147 (0.335)	-0.106 (0.488)	-0.231 (0.127)	0.305* (0.042)	-0.075 (0.625)	1									
IL-6	0.165 (0.28)	0.313* (0.03)	-0.068 (0.65)	-0.163 (0.28)	0.145 (0.34)	0.191 (0.2)	0.149 (0.329)	1								
miR 21	0.063 (0.682)	0.029 (0.849)	0.13 (0.395)	0.03 (0.845)	0.019 (0.899)	0.239 (0.114)	-0.075 (0.622)	-0.116 (0.447)	1							
miR 10b	0.066 (0.667)	-0.119 (0.438)	0.016 (0.918)	0.064 (0.677)	0.06 (0.698)	0.156 (0.305)	-0.058 (0.704)	-0.068 (0.658)	0.111 (0.468)	1						
Cyto C	0.232 (0.126)	-0.188 (0.215)	0.189 (0.213)	0.254 (0.092)	-0.052 (0.732)	-0.253* (0.043)	0.069 (0.655)	0.016 (0.918)	0.11 (0.472)	0.023 (0.879)	1					
BCL2	0.074 (0.628)	0.058 (0.705)	0.114 (0.455)	0.209 (0.168)	-0.106 (0.489)	0.317* (0.034)	0.212 (0.162)	0.14 (0.358)	0.184 (0.226)	0.049 (0.75)	0.224 (0.139)	1				
BAX	-0.094 (0.541)	-0.003 (0.982)	0.11 (0.472)	0.034 (0.825)	0.101 (0.51)	-0.005 (0.972)	-0.02 (0.897)	0.021 (0.893)	-0.033 (0.829)	0.172 (0.257)	-0.129 (0.398)	0.154 (0.314)	1			
Caspase	0.134 (0.381)	-0.138 (0.367)	0.012 (0.935)	0.101 (0.509)	-0.068 (0.659)	0.072 (0.638)	-0.145 (0.342)	0.108 (0.48)	0.006 (0.97)	0.26* (0.035)	0.083 (0.589)	0.13 (0.396)	0.183 (0.228)	1		
Procaspase	-0.058 (0.707)	-0.126 (0.41)	0.101 (0.509)	0.169 (0.268)	-0.116 (0.447)	-0.053 (0.728)	0.014 (0.925)	-0.065 (0.67)	-0.128 (0.401)	-0.115 (0.452)	0.085 (0.579)	0.236 (0.119)	0.25 (0.028)	0.213 (0.161)	1	
SMAC	-0.152 (0.319)	0.026 (0.867)	-0.036 (0.813)	-0.101 (0.51)	-0.014 (0.93)	0.07 (0.646)	-0.028 (0.855)	-0.054 (0.724)	-0.137 (0.369)	0.049 (0.751)	0.049 (0.748)	0.277 (0.05)	0.046 (0.766)	0.005 (0.971)	-0.116 (0.448)	1

*- P < 0.05, **- P < 0.0
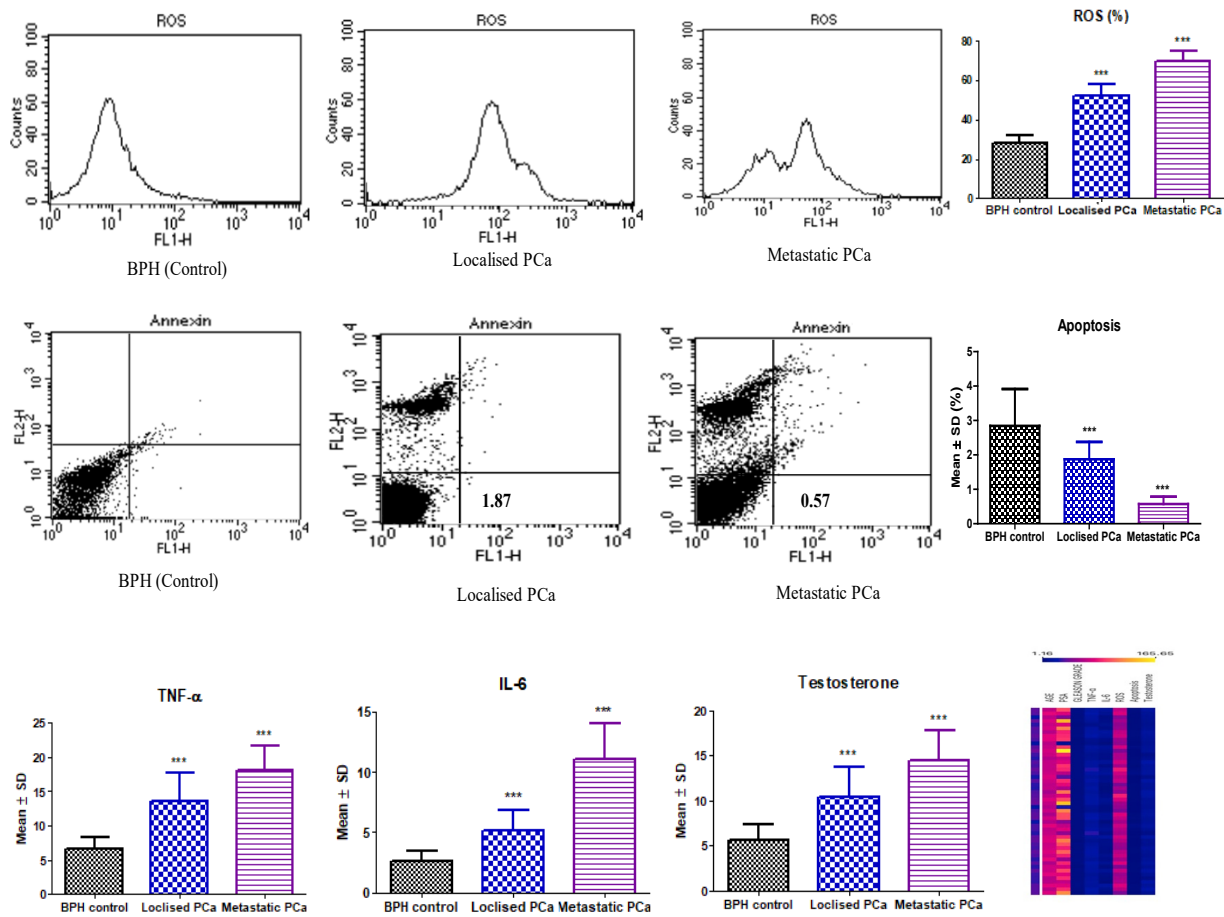
Figure 3. The Histogram Compares Mean Levels between Three Groups (ROS, Apoptosis, IL-6, TNF-α and testosterone). Comparison of mean levels between two groups (localised and metastatic as compared with BPH). P<0.05 was considered statistically significant. The heatmap depicts the fold change level of biochemical parameters in PCa. (Blue colour represents gradually increased fold change expression). *P<0.05, **P<0.01, ***P<0.001.
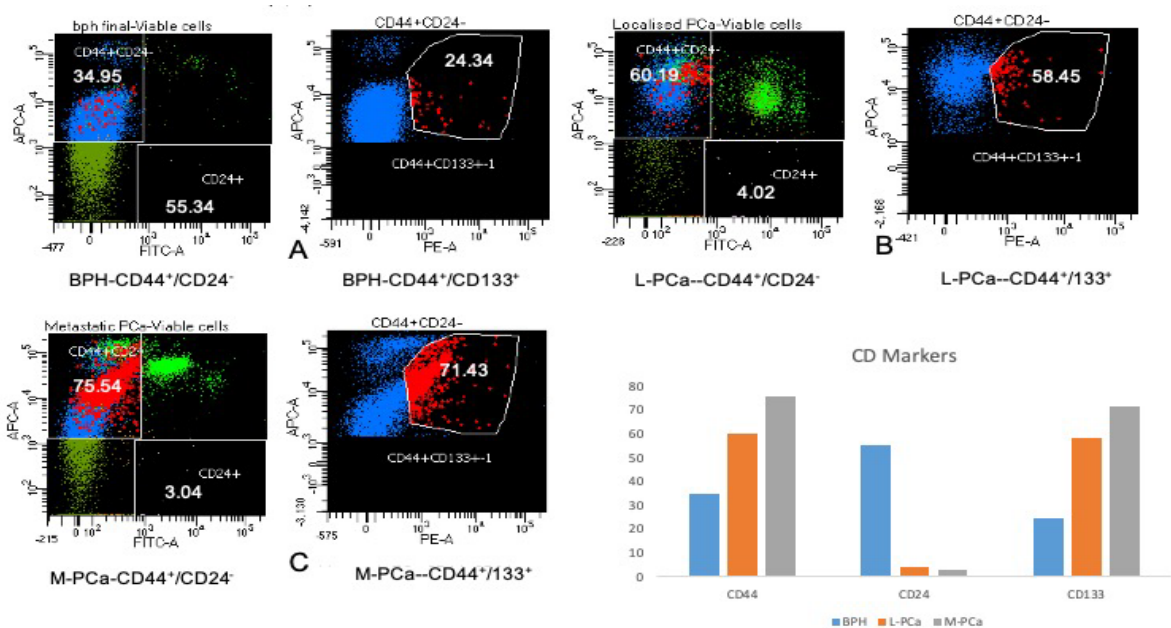

Figure 4. The Approach for Detecting CD44, CD24, and CD133 in PCa Patients' Tissue Samples in Different Groups. All normal cells were gated on a forward scatter (FSC) vs side scatter (SSC) dot plot to eliminate dead cells and debris. (A) CD44+/CD24- and CD44+/CD133+ were detected in BPH patient's tissue samples using gating cells on CD44-APC vs CD24-PE and CD 133 FITC) as a control. (B) CD44+/CD24- and CD44+/CD133+ in PCa tissue were identified in localized patients by gating cells on CD44-APC versus CD24-PE and CD133FITC. (C) In metastatic patients, CD44+/CD24- and CD44+/CD133+ PCa tissue were detected by gating cells on CD44-APC versus CD24-PE and CD133- FITC.
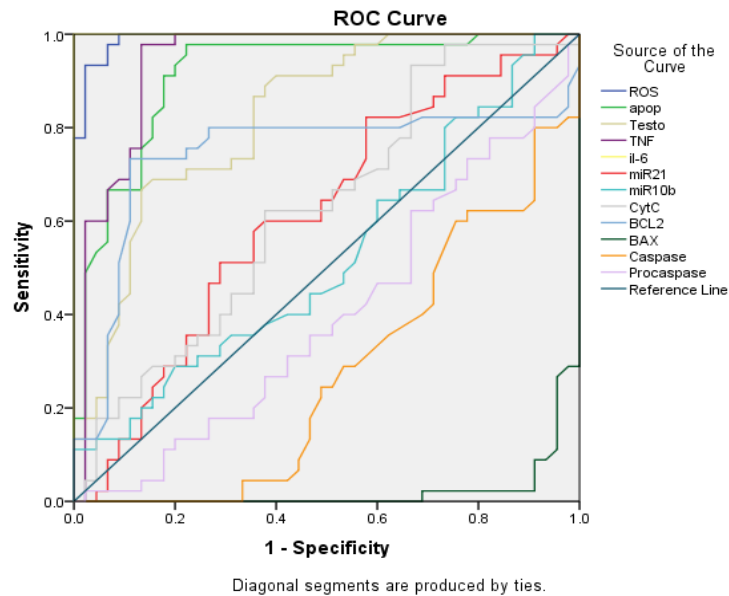
Figure 5. ROC Curve Analysis for Siagnostic Accuracy of Different Markers

Hormonal Assay

It was observed that the mean testosterone levels were considerably greater (p<0.001) in both groups, localised PCa (46.1%) (10.47±3.31) and metastatic PCa (61.0%) (14.47±3.31 ng/mL) in comparison to the BPH control group (5.65±1.70 mg/mL). Moreover, it was also significantly (p<0.001) different and elevated (27.6%) in the metastatic PCa group in comparison to the localised PCa group (Figure 3).

Cytokines

The mean TNF-α level was significant (p<0.001) and higher in both localized PCa (13.67±4.03 pg/ml) and metastatic PCa (62.8%) (18.03±3.65 pg/ml) as compared to BPH control (6.70±1.72 pg/ml). Further, it was also found significantly (p<0.001) different and higher (24.2%) in metastatic PCa in comparison to localised PCa. The IL-6 also showed a similar trend as TNF-α, i.e., the mean IL-6 was significantly (p<0.001) higher in both localized PCa (49.8%) (5.11±1.73 pg/ml) and metastatic PCa (76.9%) (11.10±2.96 pg/ml) as compared to BPH control (2.57±0.93 pg/ml). Furthermore, it was shown to be significantly (p<0.001) different and higher (54.0%) in metastatic PCa than in localised PCa (Figure 3).

Stem cell characterization result

The expression levels of CD44+/CD24- and CD44+/CD133+ were analyzed in accordance with BPH and tumor differentiation, such as localised and metastasis PCa. Our data showed that the CD44+/CD24- expression levels were significantly (p<0.001) higher in patients with localised (60.19±4.15) and metastatic PCa (75.54 ±5.45), as compared to BPH (34.93±3.45). Moreover, we found similar tends in CD44+/CD133+ both groups compared to BPH (Figure 4).

Correlation analysis

Pearson correlation examined the relation between the co-variables in metastatic PCa patients, serum PSA levels had a significant positive correlation with Gleason score (r= 0.29, p=0.01), Apoptosis (r= 0.35, p=0.02) and IL-6 levels (r= 0.313, p=0.03). Similarly, serum testosterone has a significant positive correlation with BCL2 (r= - 0.317, p=0.034) and negative correlation with the cytochrome c (r= -0.253, p=0.04). The mir-10b has a significant positive correlation with the caspase expressions (r= 0.26, p=0.03) The BCL2 has a significant positive correlation with the SMAC (r= 0.277, p=0.05). In patients with localised PCa, serum PSA levels are positively correlated with both ages of the patient (r= 0.32, p=0.031) and IL-6 levels (r= 0.36, p=0.015). The Gleason grading system has a significant negative correlation with the expression levels of Caspases (r= -0.301 p=0.024). Similarly, cytochrome C has a positive correlation with the Caspases (r=0.310, p=0.03). The miR-21 is positively correlated (r= 0.328, p=0.027) with the cytochrome C levels (Table 3 and 4).

Sensitivity and Specificity

The summaries the diagnostic accuracy (sensitivity and specificity) of various examined variables in estimating the cases of two groups of PCa patients (localised and metastatic) (Figure 7). The variables were tested alone and combined by a stepwise AIC method using regression analysis. The area under the curve (AUC) for ROS, apoptosis, testosterone TNF-α, IL-6, miR-10b, miR-21. Cyt-C, BCL2, BAX, Caspase-3 and Caspase-9 was found to be 0.99, 0.91, 0.82, 0.93, 1.0, 0.62, 0.52, 0.62,074, 0.22, 0.27 and 0.40, respectively. A pairwise comparison of ROC curves is presented in Table 5.

Prognostic and diagnostic impact of miR-10 and miR-21 in Signaling Pathways

To further explore the clinical importance of miR-10 and miR-21, as well as their association with clinical and pathological features using TCGA datasets. We used the Cancer MIRNome database to analyse the various
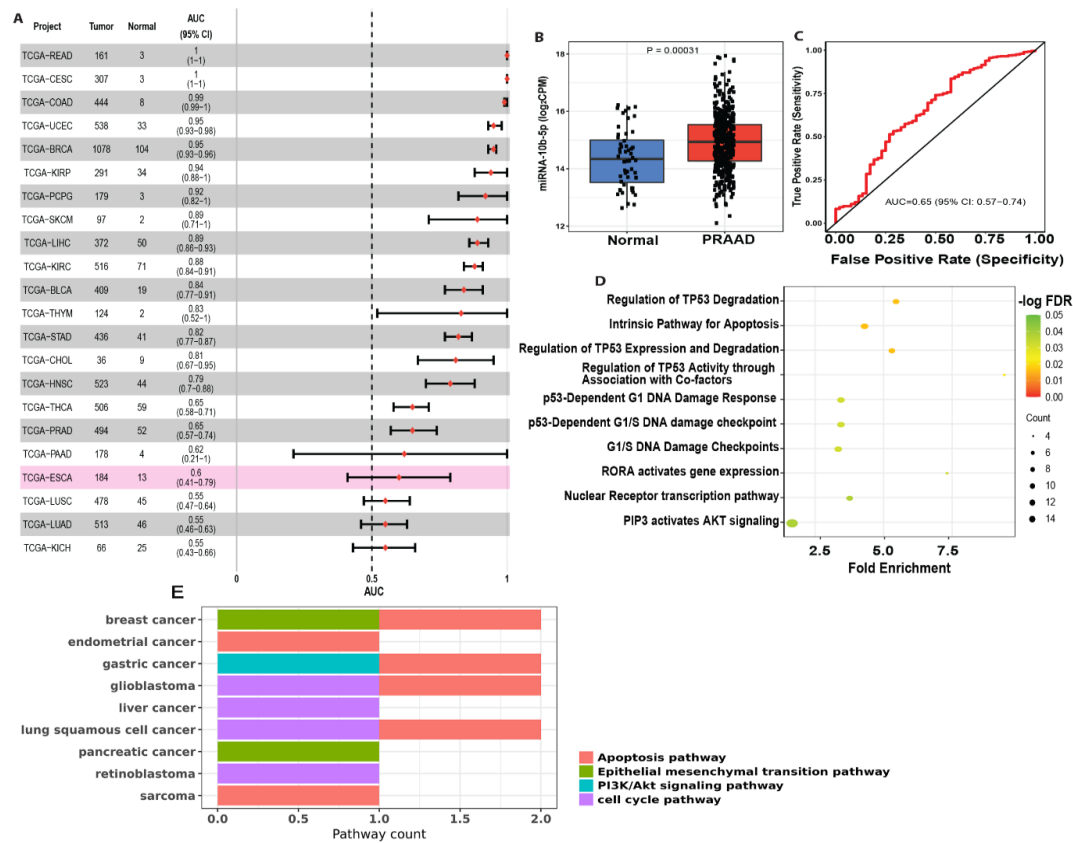
Figure 6. miR-10b-5p Expression in The Cancer Genome Atlas (TCGA) Pan-Cancer. (A) Forest plot visualizing pan-cancer survival analysis across all TCGA projects. (B) The differential expression of miR-10b-5p in TCGA of prostate cancer dataset with p value 0.00031. (C) The area under the curve (AUC) of miR-10b-5p in prostate cancer patients based on TCGA) pan-cancer, ranged from 0.57 to 0.74, proving that miR-10b-5p was an effective diagnostic molecular marker for prostate cancer. The diagnostic values of miR-10b-5p. (D) The bubble diagram of pathways enriched with related to miR-10b-5p. (E) The bar plot of pathways enrich in pan cancer.

signaling networks employed by miR-10b and miR-21. The significant correlation of the hsa-miR-10b in PCa was obtained by performing a cox regression analysis of the results from 33 types of cancer after using the Cancer MIRNome database's TCGA pan-cancer section (Figure 6A). Further, correlation analysis was done to compare

Table 5. Diagnostic Accuracy of Different Markers in the Diagnosis of Localized PCa and Metastatic PCa Cases Using ROC Curve Analysis

Test Result Variable(s)	Area Under the Curve				
	Area	Std. Errora	Asymptotic Sig.b	Asymptotic 95% Confidence Interval	
				Lower Bound	Upper Bound
ROS	0.992	0.006	0	0.979	1
apop	0.914	0.031	0	0.852	0.975
Testo	0.825	0.044	0	0.739	0.91
TNF-α	0.939	0.028	0	0.885	0.993
IL-6	1	0	0	1	1
miR21	0.613	0.06	0.065	0.496	0.73
miR10b	0.523	0.061	0.71	0.402	0.643
Cyt-C	0.625	0.059	0.042	0.509	0.74
BCL2	0.742	0.059	0	0.626	0.858
BAX	0.022	0.012	0	0	0.045
Caspase-3	0.278	0.053	0	0.174	0.382
Caspase-9	0.4	0.06	0.102	0.283	0.517

The test result variable(s): apop, Testo, TNF, miR21, miR10b, CytC, BCL2, BAX, Caspase-3 and Caspase-9 has at least one tie between the positive actual state group and the negative actual state group. Statistics may be biased; a, Under the nonparametric assumption; b, Null hypothesis: true area = 0.5
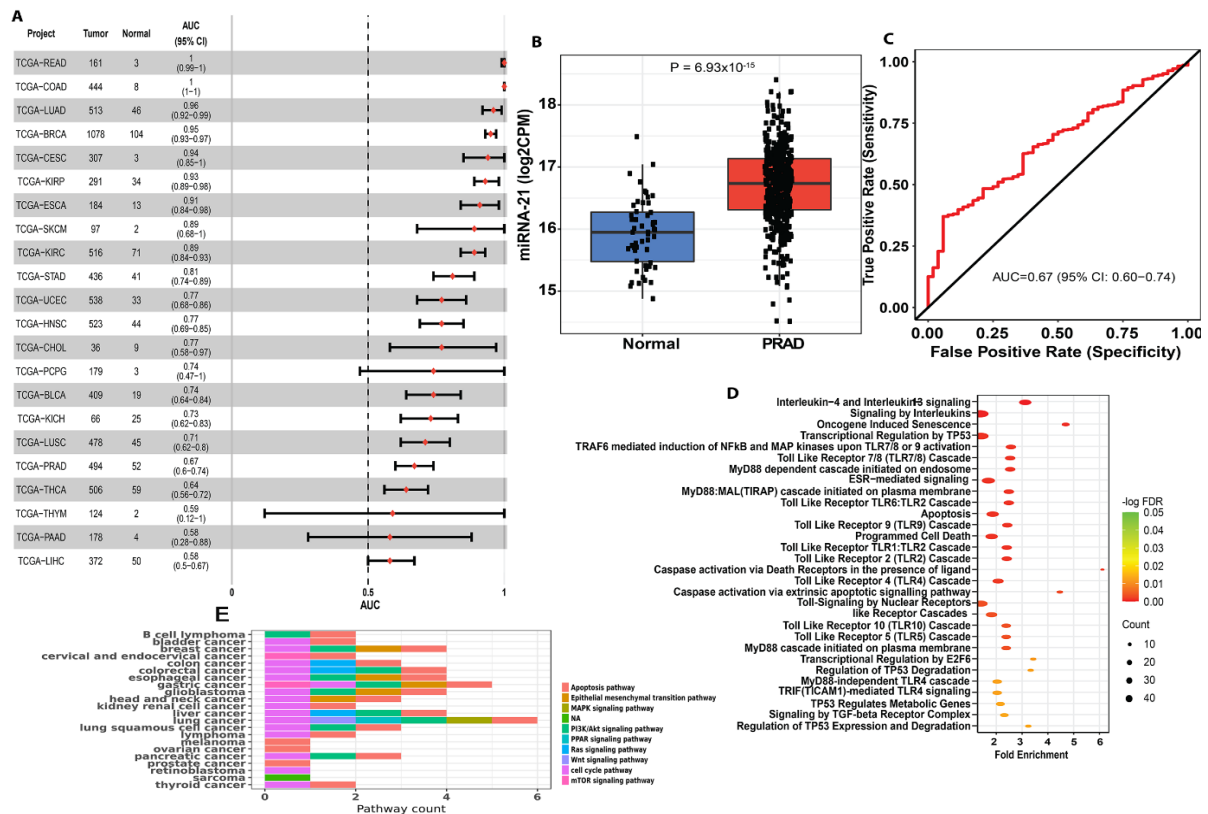
Figure 7. miR-21 Expression in The Cancer Genome Atlas (TCGA) Pan-Cancer. (A) Forest plot visualizing pan-cancer survival analysis across all TCGA projects. (B) The differential expression of miR-21 in TCGA of prostate cancer dataset with high significant p-value. (C) The area under the curve (AUC) of miR-21-3p in prostate cancer patients based on TCGA) pan-cancer, ranged from 0.60 to 0.74, proving that miR-21 was an effective diagnostic molecular marker for prostate cancer. The diagnostic values of miR-21. (D) The bubble diagram of pathways enriched with related to miR-21. (E) The bar plot of pathways enrich in pan cancer.

the relation of miR-10b expression in the PCa and other organ cancers. We found that the expression of miR-10b was different in various cancers. As per results obtained from TCGA samples and the Cancer MIRNome website, the expression of miR-10b was significantly higher in PCa in comparison to healthy controls (P=0.00031) (Figure 6B). As per the ROC analysis obtained in the TCGA pan-cancer cancer MIRNome, PCa was found to have an AUC value of 0.65 (95% CI: 0.57–0.74) among adjacent normal tissues (Figure 6C). Thus, these results proved the significant impact of the hsa-miR-10b expression in the diagnosis of PCa. Using the miRNA Cancer MAP database, it was also found that these miRNAs with signaling networks were involved in tumor progression in prostate cancer. The apoptotic activity and association of miR-10b with the cell cycle and p53 signaling regulatory network were also surveyed (Figure 6D). The impact of miR-10b in other cancers like breast, lung, endometrial, and liver was also studied, revealing its significant role in these cancers (Figure 5E).

The significant correlation of the hsa-miR-21 in PCa was also obtained after performing cox regression analysis on pan-cancer (Figure 7A). Moreover, a correlation analysis was done, and the relationship of miR-21 expression in prostate cancer was compared with other cancers. The results obtained from TCGA samples and the

Cancer MIRNome website revealed that the expression of miR-21 was significantly higher in PCa tissue compared to healthy control tissue (P=6.93x10-15) (Figure 7B). As per the ROC analysis obtained in the TCGA pan-cancer of Cancer MIRNome, PCa was found to have an AUC value of 0.67 (95% CI: 0.60–0.74) compared to the adjacent tissue (Figure 7C). Thus, together these results proved the significant impact of hsa-miR-21 expression in the diagnosis of PCa. The analysis also included apoptotic activity and the association of miR-21 with the cell cycle and p53 signaling regulatory network (Figure 7D). Likewise, the role of miR-21 in other cancers, including breast, lung, endometrial, and liver cancers, was also studied (Figure 7E).

Discussion

PCSCs are a small, dynamic, and heterogeneous population of self-renewable cancer cells, leading to tumour growth and development (Zuoren et al., 2012). There is mounting data from multiple studies that suggest an increase in CSCs in tumour tissue may be linked to therapeutic failure (Abrahamsson et al., 1999). The CSCs were identified and isolated using different cell surface markers and transcription factors. Many such markers have been identified in PCa, such as CD24, CD44,
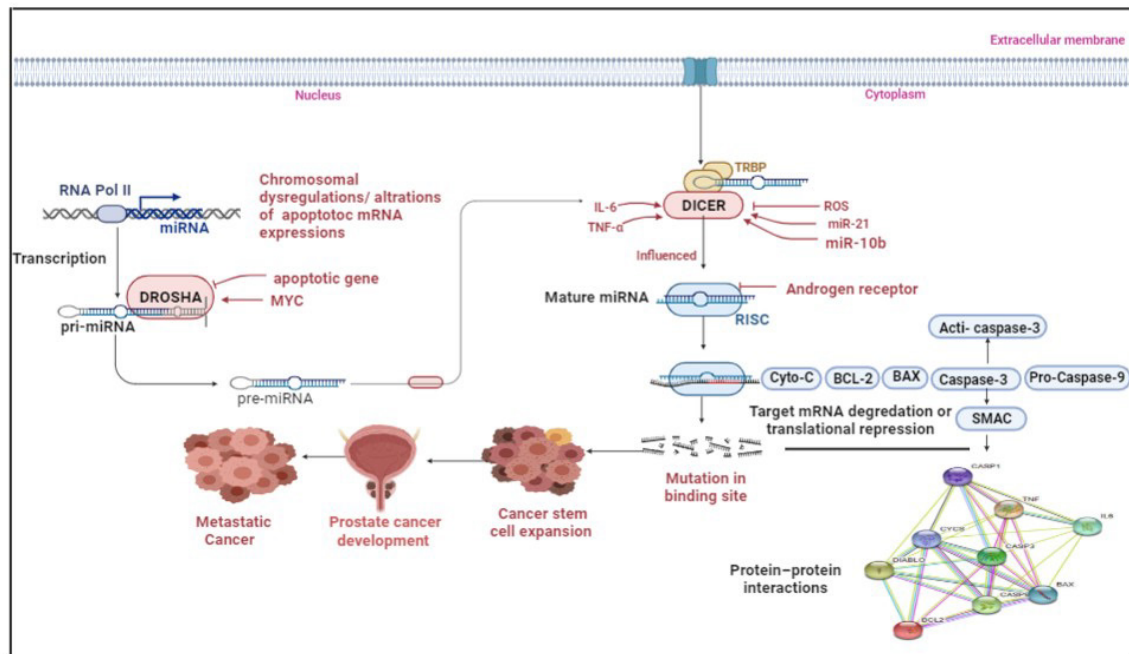
Figure 8. Schematic Representation of the Pathway Influencing the Progression and Remission of PCa through the Apoptotic Pathway and Prostate Cancer Stem Cell. miR-21 and miR-10b target the expression of genes in the apoptotic pathway. The increased expression of these miRNAs leads to alteration of apoptotic pathway genes and increases the cell transformation into Cancerous stem cells. The suppression of apoptosis and the induction of stemness lend the prostate cancer metastatic ability and culminate in more severe phenotypes.

CD133 (prominin-1), CD166 (Activated Leukocyte Cell Adhesion Molecule), and α2β1 integrin (Mei et al., 2019). Despite multiple markers, have not yet elucidated the right combination that could precisely characterize CSCs, because of PCa genetic heterogeneity. In a recent study, Patrawala et al., (2006) showed that a large proportion of prostate cell line-derived CD44+ cells comprised tumour progenitor cells and stated that around 70% of the CD44+ also have CD133+. Similarly, Collins et al., (2005) also demonstrated that CD44+ and CD133+ cells from PCa patients are highly tumorigenic. In this study, we have used the combination of CD44+/CD24- and CD44+/CD133+ to identify these PCSCs. Consistent with the above reports, both localized PCa and metastatic PCa from our study had increased expression of CD44+/CD24− and CD44+/CD133+ (Figure 4). Several studies have highlighted the role of CD44+/CD24− and CD133+ stem cell markers to distinguish cancer cell that transforms into highly aggressive mature tumour cells (Collins et al., 2005).

Cancers have been demonstrated to have altered patterns of miRNAs (Raue et al., 2021; Carthew et al., 2009). In this study, we assessed the expression of miRNA-10b and miRNA-21 and found that miR-10b and miR-21 expression were significantly increased in both localized and metastatic PCa compared to the BPH (Figure 2). Growing evidence suggests that altered expression of miR-10b plays a vital role in advancing and spreading multiple malignancies such as breast cancer, gastric cancer, and lung cancer through various mechanisms (Patrick et al., 2018). Notably, miR-10b promotes CSCs-like property are essential characteristics associated with metastasis cancer (Sheedy et al., 2018). Also, some studies have demonstrated that the upregulated

miR-10b was correlated with increased lymph node metastasis, advanced clinical stage, and shortened survival rate in various types of cancers (Collins et al., 2018). Similarly, miR-21 was overexpressed in metastatic cancer, functioning as a regulator of tumour suppressor genes and apoptotic genes, such as the transformation suppressor programmed cell death protein 4 (PDCD4) (Ribas et al., 2010). Previous studies have also demonstrated the anticoagulant and anti-apoptotic effects of miR-21 in disrupting the apoptosis pathway and facilitating cancer cell survival (Liu et al., 2019).

The various targets of miRNAs enable the regulation of a wide range of cellular pathways and signaling cascades (Carthew et al., 2009). In silico target analysis was performed for both miRNAs in PCa, and identified targets included common apoptosis-regulating genes (table 2). Thus, based on the above analysis, the mRNA expression of apoptotic genes was assessed to understand the role of miRNAs in regulating apoptotic gene expression (BCL-2, BAX, Caspase-3, Caspase-9, Cytochrome C, and SMAC) in a different stage of PCa. The study results showed cytochrome C and BCL-2 genes to have a higher expression in localised and metastatic PCa than in BPH. In contrast, BAX, Caspase-3, Caspase-9, and SMAC were expressed in lower quantities in localised and metastatic PCa as compared to BPH. Interestingly, the dysregulation of BCL-2 and SMAC levels provokes mitochondrial cytochrome C to be released into the cytosol, causing activation of caspase-3 (Hasenjäger et al., 2004). Collectively, our observations strongly suggest that altered apoptotic gene expressions lead to an imbalance between cell division and death, which appears crucial for PCa development. There is abundant

evidence to support that members of the BCL-2 group are vital for the apoptotic regulation of PCa (Suvarna et al., 2019). However, the BCL-2 oncoprotein, encoded by the BCL-2 proto-oncogene, has been linked to cell survival by suppressing programmed cell death (Suvarna et al., 2019). Furthermore, recent evidence supports that BCL-2 has a dominant role in hormone resistance in PCa (Hasenjäger et al., 2004). Interestingly, SMAC seems to bypass the need to release cytochrome c by directly activating caspase and acts as a sensitizer for mitochondrial activation of the caspase and apoptosis (Hasenjäger et al., 2004; Devarajan et al., 2002).

In our study, we also observed a significantly decreased expression of caspase-3 and apoptosis in patients with localised and metastatic PCa, compared to those with BPH. However, caspase-9 was found to be decreased in metastatic groups only as compared to BPH. Surprisingly, intrinsic pathway of apoptosis has caspase-9 as the initiator, and caspase 3 plays the role of an "executor" enzyme (Devarajan et al., 2002). Malignant cells have been shown to have reduced apoptosis due to an imbalance of pro-apoptotic and anti-apoptotic proteins, resulting in reduced caspase-3 function. There is evidence that low caspase-3 promotes carcinogenesis and contributes to the progression of various cancers such as colorectal, breast and PCa (Hasenjäger et al., 2004). Our study also assessed the clinical outcomes with the patient survival information, miRNA expression profiles and gene expression profiles for PCa through miRNA-mRNA interaction analysis. We identified miRNA-mRNA pairs with an inverse correlation that have significant differences in survival between patient groups. Despite this, our findings were consistent with genomic expression from TCGA datasets, as well as survival analysis of miRNAs (Figures 6 and 7) and gene expressions. (See Supplementary Figures 1 and 4).

Reactive oxygen species (ROS) and various inflammatory cytokines are always elevated in malignancies (Westaby et al., 2021). However, the biological significance of the interplay between ROS and inflammatory cytokine still remains elusive. We found a significant elevation in ROS levels in the localized and metastatic patients compared with BPH. Increased ROS levels enhanced the oxidative damage in biomolecules and accentuated the pathogenesis and progression of PCa (Westaby et al., 2021). In this study, the serum IL-6 and TNF-α levels were increased in both metastatic and localized PCa patients compared with BPH (Figure 3). There was a significant association between the serum cytokines levels, staging of disease, and metastasis. Recent studies have revealed that the increased levels of IL-6 play a vital role in PCa pathogenesis, and TNF-α stimulates apoptotic cell death through accelerated IL-6 production of PCa (Michalaki et al., 2019). This paradox is associated with activating multiple anti-apoptotic genes, including the TNF-α family of paracrine and autocrine loop transcription factors that influence the activity of PCa (Hsieh et al., 2022). An exocrine gene product of the prostate has been characterized that interacts with its androgen receptor (AR) in prostate cells, which regulates expansion and characterization (Sharifi et al., 2005).

Interestingly, IL-6 plays a vital role in the evolution

and advancement of CRPC (Ene et al., 2022). Similarly, TNF-α is also insensitive in these androgen-insensitive cells and simultaneously triggers cell survival and cell death due to the constitutive activation of anti-apoptotic genes (Perez et al., 2000). The ROC curve analysis showed significant diagnostic AUCs for ROS, IL-6, BAX, BCL-2, apoptosis, and testosterone, which significantly improved the existing clinical parameters (localised and metastatic stage) (Table 5). The results of this study emphasized that miR-10b and miR-21 may be used as a therapeutic target for anti-metastatic treatment or as a prognostic marker for early identification. The rationale and selection criteria for treating early stage or metastatic PCa with the miR-10b antagomir or mimic miR as a component of a neoadjuvant regimen might also be determined by measuring the expression of miR-21 and miR-10b. The current study also recommended more research into the relationship between miR-21 and miR-10b and PCa stage. To corroborate our findings and examine the relationships between clinical factors including tumour subtypes, type of cell tumour, hormone status, and clinical pathology, with a larger sample size should be carried out. Further, functional assays for stemness and protein level evaluation of apoptosis-related genes should be done.

In conclusion, In this study, we identified the involvement of miR-10b and miR-21 and apoptotic pathway mRNAs expression in PCa. Collectively, our findings reveal that increased expression of these miRs in PCa leads to defective expression of the genes in the apoptotic pathway, increased PCSCs, and the production of an excess of cytokines, free radicals, and testosterone (Figure 8). To our knowledge, this is the first study to investigate the miR-10b and miR-21 and their associations with the apoptotic genes and PCSCs in different stages of PCa. Although the links between miR-10b and miR-21 and stemness is not directly assessed, our findings indicate that miR-10b and miR-21 likely target apoptotic genes with crucial roles in PCa pathogenesis may help in early PCa diagnosis. However, further in-vitro studies will be required to validate the actual function of miR-10b and miR-21 in PCa.

Author Contribution Statement

Acknowledgements

Biochemistry and Urology at the All-India Institute of Medical Science (AIIMS), Jodhpur, India as per principles of Declaration of Helsink, after receiving ethical approval from the AIIMS Institutional Human Ethics Committee (AIIMS/RES (04)/2017/219). Each subject gave written informed consent after accepting a thorough written and verbal explanation of the study.

Availability of data and materials

Data sets are available with the corresponding authors and will be shared on reasonable request.

Conflict of interest

All authors have read, approved, and agree with the manuscript's content. The authors of the manuscript also have no conflict of interest.

References

Abrahamsson PA (1999). Neuroendocrine cells in tumour growth of the prostate. *Endocr Relat Cancer*, **6**, 503-19.

Alvarez ML, Doné SC (2014). SYBR® Green and TaqMan® quantitative PCR arrays: expression profile of genes relevant to a pathway or a disease state. *Methods Mol Biol,* **1182**, 321-59.

Bray F, Ferlay J, Soerjomataram I, et al (2018). Global cancer statistics 2018: GLOBOCAN estimates of incidence and mortality worldwide for 36 cancers in 185 countries. *CA Cancer J Clin*, **68**, 394-424.

Carthew RW, Sontheimer EJ (2009). Origins and Mechanisms of miRNAs and siRNAs. *Cell*, **136**, 642-55.

Collins AT, Berry PA, Hyde C, et al (2005). Prospective identification of tumorigenic prostate cancer stem cells. *Cancer Res*, **65**, 10946-51.

Culig Z (2021). Interleukin-6 Function and Targeting in Prostate Cancer. *Adv Exp Med Bio*, **l1290**, 1-8.

Devarajan E, Sahin AA, Chen JS, et al (2002). Down-regulation of caspase 3 in breast cancer: a possible mechanism for chemoresistance. *Oncogene*, **21**, 8843-51.

Ene CV, Nicolae I, Geavlete B, et al (2022). IL-6 Signaling Link between Inflammatory Tumor Microenvironment and Prostatic Tumorigenesis. *Anal Cell Pathol (Amst)*, **2022**, 5980387.

Gao Z, Liu H, Shi Y, et al (2019). Identification of Cancer Stem Cell Molecular Markers and Effects of hsa-miR-21-3p on Stemness in Esophageal Squamous Cell Carcinoma. *Cancers*, **11**, 518.

Hasenjäger A, Gillissen B, Müller A, et al (2004). Smac induces cytochrome c release and apoptosis independently from Bax/BCL-x(L) in a strictly caspase-3-dependent manner in human carcinoma cells. *Oncogene*, **23**, 4523-35.

Hering FL, Lipay MV, Lipay MA, et al (2001). Comparison of positivity frequency of bcl-2 expression in prostate adenocarcinoma with low and high Gleason score. *Sao Paulo Med J*, **119**, 138-41.

Hsieh HL, Yu MC, Cheng LC, et al (2022). Quercetin exerts anti-inflammatory effects via inhibiting tumor necrosis factor-α-induced matrix metalloproteinase-9 expression in normal human gastric epithelial cells. *World J Gastroenterol*, **28**, 1139-58.

Hurt EM, Kawasaki BT, Klarmann GJ, et al (2008). CD44+CD24− prostate cells are early cancer progenitor/stem cells that provide a model for patients with poor prognosis. *Br J Cancer*, **98**, 756-65.

Khan AQ, Ahmed EI, Elareer NR, et al (2019). Role of

miRNA-Regulated Cancer Stem Cells in the Pathogenesis of Human Malignancies. *Cells*, **8**, 840.

Liu HY, Zhang YY, Zhu BL, et al (2019). miR-21 regulates the proliferation and apoptosis of ovarian cancer cells through PTEN/PI3K/AKT. *Eur Rev Med Pharmacol Sci*, **23**, 4149-55.

Livak KJ, Schmittgen TD (2001). Analysis of relative gene expression data using real-time quantitative PCR and the 2(-Delta Delta C (T)) Method. *Methods*, **25**, 402-8.

Mathur P, Sathishkumar K, Chaturvedi M, et al (2020). ICMR-NCDIR-NCRP Investigator Group. Cancer Statistics, 2020: Report From National Cancer Registry Programme, India. *JCO Glob Oncol*, **6**, 1063-75.

Mei W, Lin X, Kapoor A, et al (2019). The Contributions of Prostate Cancer Stem Cells in Prostate Cancer Initiation and Metastasis. *Cancers (Basel)*, **11**, 434.

Michalaki V, Syrigos K, Charles P, Waxman J (2004). Serum levels of IL-6 and TNF-α correlate with clinicopathological features and patient survival in patients with prostate cancer. *Br J Cancer*, **90**, 2312–6.

Morote J , Planas J, Ramirez C, et al (2010). Evaluation of the serum testosterone to prostate-specific antigen ratio as a predictor of prostate cancer risk. *BJU Int*, **105**, 481-4.

Patrawala L, Calhoun T, Schneider-Broussard R, et al (2006). Highly purified CD44+ prostate cancer cells from xenograft human tumors are enriched in tumorigenic and metastatic progenitor cells. *Oncogene*, **25**, 1696-708.

Patrick Sheedy, Zdravka Medarova (2018). The fundamental role of miR-10b in metastatic cancer. *Am J Cancer Res*, **8**, 1674-88.

Perez D, White E (2000). TNF-alpha signals apoptosis through a bid-dependent conformational change in Bax that is inhibited by E1B 19K. *Mol Cell*, **6**, 53-63.

Raue R, Frank AC, Syed SN, et al (2021). Therapeutic Targeting of MicroRNAs in the Tumor Microenvironment. *Int J Mol Sci*, **22**, 2210.

Ribas J, Lupold SE (2010). The transcriptional regulation of miR-21, its multiple transcripts, and their implication in prostate cancer. *Cell Cycle*, **9**, 923-9.

Rupaimoole R, Slack FJ (2017). MicroRNA therapeutics: towards a new era for the management of cancer and other diseases. *Nat Rev Drug Discov*, **16**, 203-22.

Sharifi N, Gulley JL, Dahut WL (2005). Androgen deprivation therapy for prostate cancer. *JAMA*, **294**, 238-44.

Sheedy P, Medarova Z (2018). The fundamental role of miR-10b in metastatic cancer. *Am J Cancer Res*, **8**, 1674-88.

Shukla KK, Agnihotri S, Gupta A, et al (2013). Significant association of TNFα and IL-6 gene with male infertility--an explorative study in Indian populations of Uttar Pradesh. *Immunol Lett*, **156**, 30-7.

Shukla KK, Misra S, Pareek P (2017). Recent scenario of microRNA as diagnostic and prognostic biomarkers of prostate cancer. *Urol Oncol*, **35**, 92-101.

Siegel R, Miller K, Jemal A, Cancer Statistics (2020). *CA Cancer J Clin*, **70**, 7-30.

Sticht C, De La Torre C, Parveen A, Gretz N (2018). miRWalk: An online resource for prediction of microRNA binding sites. *PLoS One*, **13**, e0206239.

Suvarna V, Singh V, Murahari M (2019). Current overview on the clinical update of BCL-2 anti-apoptotic inhibitors for cancer therapy. *Eur J Pharmacol*, **862**, 172655.

Szklarczyk D, Gable AL, Nastou KC, et al (2021). The STRING database in 2021: customizable protein-protein networks, and functional characterization of user-uploaded gene/measurement sets. *Nucleic Acids Res*, **49**, 605-12.

Tang Z, Li C, Kang B, et al (2017). GEPIA: a web server for cancer and normal gene expression profiling and interactive

analyses. *Nucleic Acids Res*, **45**, 98-102.

Unberath P, Mahlmeister L, Reimer N, et al (2022). Searching of Clinical Trials Made Easier in cBioPortal Using Patients' Genetic and Clinical Profiles. *Appl Clin Inform*, **13**, 363-9.

Vermes I, Haanen C, Steffens-Nakken H, Reutelingsperger C (1995). A novel assay for apoptosis, flow cytometric detection of phosphatidylserine expression on early apoptotic cells using fluorescein-labelled annexin V. *J Immunol Methods*, **184**, 39-45.

Westaby D, Jimenez-Vacas JM, Padilha A, et al (2021). Targeting the Intrinsic Apoptosis Pathway: A Window of Opportunity for Prostate Cancer. *Cancers (Basel)*, **14**, 51.

Xiao J, Cohen P, Stern MC, et al (2018). Mitochondrial biology and prostate cancer ethnic disparity. *Carcinogenesis*, **39**, 1311-9.

Yun EJ, Zhou J, Lin CJ, et al (2016). Targeting Cancer Stem Cells in Castration-Resistant Prostate Cancer. *Clin Cancer Res*, **22**, 670-9.

Zuoren Yu, Timothy G. Pestell, et al (2012). Pestell, Cancer stem cells. *Int J Biochem Cell Biol*, **44**, 2144-51.